

UNCLASSIFIED

Defense Technical Information Center
Compilation Part Notice

ADP023555

TITLE: High Resolution Simulations of Arctic Sea Ice, 1979-1993

DISTRIBUTION: Approved for public release, distribution unlimited

This paper is part of the following report:

TITLE: Proceedings of the Workshop on Sea Ice Extent and the Global Climate System Held in Toulouse, France on April 15-17, 2002

To order the complete compilation report, use: ADA471691

The component part is provided here to allow users access to individually authored sections of proceedings, annals, symposia, etc. However, the component should be considered within the context of the overall compilation report and not as a stand-alone technical report.

The following component part numbers comprise the compilation report:

ADP023547 thru ADP023559

UNCLASSIFIED

High resolution simulations of Arctic sea ice, 1979–1993

Wieslaw Maslowski & William H. Lipscomb



To evaluate improvements in modelling Arctic sea ice, we compare results from two regional models at $1/12^\circ$ horizontal resolution. The first is a coupled ice–ocean model of the Arctic Ocean, consisting of an ocean model (adapted from the Parallel Ocean Program, Los Alamos National Laboratory [LANL]) and the “old” sea ice model. The second model uses the same grid but consists of an improved “new” sea ice model (LANL/CICE) with a simple ocean mixed layer. Both models are forced with European Centre for Medium-range Weather Forecasts reanalysis data for 1979–1993. A comparison of the two sea ice models focuses on the winter of 1987 to emphasize the internal ice stress and to minimize biases towards a particular Arctic climate regime. The “new” sea ice model gives improved ice deformation and drift fields. These improvements are associated at least in part with the multi-category representation of the ice thickness distribution and more realistic parameterization of the ice strength. Long, narrow features in ice divergence and shear fields resemble those observed in SAR imagery, except that their average width is overestimated, possibly due to insufficient horizontal resolution. We also compare the mean sea ice drift and its decadal variability in two “old” sea ice models at different horizontal resolutions: 18-km and 9-km. We find no significant change in ice drift between the two models, except in areas of significant ice–ocean interactions due to more realistic ocean currents and water mass properties in the 9-km model.

W. Maslowski, Dept. of Oceanography, Naval Postgraduate School, 833 Dyer Rd., Monterey, CA 93943, USA, maslowsk@nps.navy.mil; W. H. Lipscomb, T-3 Fluid Dynamics Group, Los Alamos National Laboratory, Los Alamos, NM 87545, USA.

With its sea ice cover, the Arctic Ocean has been difficult to model in both global climate simulations and regional studies. One challenge is to represent faithfully the physical processes specific to sea ice and oceans in polar regions. Another challenge, intimately linked to the first, is to resolve small-scale features such as narrow boundary currents (0[100km]), the Rossby radius of deformation (0[10km]), and the bottom bathymetry and land geometry controlling the physics and inter-basin/inter-ocean communications. Climate change studies suggest that the Arctic is highly sensitive to greenhouse warming, largely because of positive feedbacks associated with thinning and retreat of the insulating, highly

reflective sea ice cover. The ice models in these studies have typically been run at fairly coarse resolution ($\sim 3^\circ$), using crude parameterizations of the thermodynamic and dynamic processes that determine the ice thickness and extent. However, recent advances in sea ice modelling, together with parallel supercomputers for high resolution modelling, make it feasible to improve the fidelity of Arctic Ocean simulations and thereby increase the reliability of climate change predictions.

In this paper we present results from two regional models of the Arctic Ocean at 9-km (or $1/12^\circ$) resolution. We briefly describe the ice and ocean models, atmospheric forcing, and initial and boundary conditions used in this study.

We then compare model results, focusing on sea ice concentration, velocity, shear and divergence fields that can be qualitatively compared to similar sea ice products available from high resolution SAR imagery, such as the RADARSAT Geophysical Processor System (RGPS) analyses (e.g. Kwok 2001). To better understand model improvements following from increased resolution, we also compare the mean sea ice drifts and anomalies from our earlier 18-km and 30 level coupled ice–ocean model (Maslowski et al. 2001) with the similar coupled model run at 9-km with 45 ocean levels. We conclude by discussing possible sources of model differences and suggesting further experiments. Due to length constraints in this publication, only limited presentation of the results is possible.

Model Description

Coupled ice–ocean model

The 9-km model uses a parallel version of the basic sea ice model of Hibler (1979), with viscous-plastic dynamics, simple thermodynamics and two thickness categories (thick ice and thin ice/open water). The ice model is coupled to a regional adaptation of the Parallel Ocean Program (POP) of Los Alamos National Laboratory (LANL). This ocean model has a free-surface formulation (Smith et al. 1992) and 45 vertical levels. The model domain is defined in a rotated spherical coordinate system to eliminate the singularity at the North Pole and was chosen to include all the northern ice-covered oceans. It extends from the North Pacific at $\sim 30^\circ\text{N}$, across the central Arctic and sub-Arctic seas, into the North Atlantic to $\sim 45^\circ\text{N}$. The model uses significantly improved bathymetry data, including the 2.5 km resolution International Bathymetric Chart of the Arctic Ocean database (Jakobsson et al. 2000), along with the recently upgraded monthly mean temperature and salinity climatology (PHC) from the University of Washington (Steele et al. 2001). The model includes run-off from most major rivers (the Yukon, Mackenzie, Dvina, Pechora, Ob, Yenisey, Kotuoy, Lena, Kolyma and Indigirka) as well as ungauged run-off. Other model formulations are similar to those used in the 18-km, 30-level coupled ice–ocean model of the Arctic Ocean of Maslowski et al. (2000).

We have so far completed a 63-year integration of the coupled 9-km ice–ocean model. The model

was forced with daily-average atmospheric fields (downward longwave and shortwave radiation, air temperature and density, specific humidity, precipitation, and wind velocity) from the European Centre for Medium-range Weather Forecasts (ECMWF) 1979–1993 reanalysis. Surface fluxes of turbulent heat and momentum were computed using bulk formulas. Following the 27-year spinup, we performed an additional 21-year run using the repeated 1979 ECMWF annual cycle for the first 6 years and 1979–1981 inter-annual fields for the last 15 years. In this way we forced the sea ice and ocean toward conditions of the late 1970s and early 1980s, which were used to start the 1979–1993 integration.

CICE model

The “new” sea ice model, CICE version 3.0 (Hunke & Lipscomb 2001), was developed at LANL for climate studies and differs from the old Hibler model in several respects. The new ice model incorporates the latest version of the elastic-viscous-plastic (EVP) dynamics of Hunke & Dukowicz (1997), which reduces to the viscous-plastic model at long time scales but uses elastic waves to improve the response on short time scales and increase computational efficiency. The wind stress depends not only on the wind velocity, but also on a drag coefficient that varies with the boundary layer stability following Bryan et al. (1996). (The old ice model uses a constant drag coefficient.) Vertical heat transfer and growth and melting of ice and snow are computed using the multi-layer energy-conserving thermodynamic model of Bitz & Lipscomb (1999), which includes a temperature-dependent heat capacity to mimic brine pocket effects. The ice is transported horizontally using the incremental remapping scheme of Lipscomb & Hunke (unpubl. ms), which is second-order accurate in space except where the accuracy is reduced locally to preserve monotonicity. The old model uses a second-order centred difference scheme that requires a diffusion term to maintain numerical stability.

Perhaps the most important difference is that the new model has multiple ice thickness categories (along with open water). Ice is transferred between categories as it grows and melts using the thickness-remapping scheme of Lipscomb (2001). Several studies (e.g. Maykut 1982; Bitz et al. 2001) have shown that the ice strength, heat exchange with the atmosphere, and other

properties are sensitive to the ice thickness distribution, especially to the amount of thin first-year ice. With multiple categories, sea ice ridging can be represented as a process that moves ice from thin categories to thicker categories, as suggested by Thorndike et al. (1975) and Hibler (1980). In the new model the ice strength P is proportional to the increase in potential energy during ridging, following Rothrock (1975). In the old model the strength is represented as:

$$P = P^* h \exp[-C(1-A)],$$

where h is the mean ice thickness, A is the open water fraction, and P^* and C are empirical constants that are tuned to give reasonable ice strengths. Following Hibler (1979), we set $P^* = 27\,500 \text{ N/m}^2$ and $C = 20$. In both parameterizations, the ice weakens as the open water fraction increases. In the old model, however, the ice strength depends on the mean ice thickness, whereas in the new model, the ice strength depends on the amount and thickness of thin ice.

We have completed a 20-year integration of CICE on the 9-km grid. The run consists of a 10-year spinup and a 10-year interannual run forced with the ECMWF 1979–1988 reanalysis data. The model was run with five ice thickness categories, each having four vertical ice layers and one snow layer, and other standard parameters as described in Hunke & Lipscomb (2001). The ice was coupled not to a full ocean model, but to a simple ocean mixed layer that can absorb heat and grow ice in leads. The ice receives heat from the ocean at its bottom surface, although not as much as in coupled models where there can be an upward heat flux from beneath the mixed layer. Also, the ocean velocity is set to zero in the water stress term of the sea ice momentum equation. We emphasize that disparities in sea ice behaviour between the old and new models could arise not only from differences in the ice models themselves, but also from different coupling to the ocean and atmosphere. In the near future we plan to couple CICE with POP so as to make more detailed comparisons of the old and new ice models. The stand-alone integration, however, already reveals significant differences between the two ice models.

Results

To differentiate the effects of a new ice model

from those of increased spatial resolution, we first compare sea ice drift in two coupled ice–ocean models of the Arctic Ocean, both using the “old” ice model but at different resolution. The coarser model, with an 18-km grid and 30 vertical levels, extends from (closed) Bering Strait to $\sim 45^\circ\text{N}$ in the North Atlantic. Maslowski et al. (2001) have shown that the mean sea ice drift in this model changes its circulation over a 10-year period between 1981–82 and 1991–92. In the 1980s the large-scale anticyclonic Beaufort Gyre prevails, with the Transpolar Drift positioned along the Lomonosov Ridge (Fig. 2a in Maslowski et al. 2001). In the early 1990s the Beaufort Gyre shrinks to occupy only the Beaufort Sea, and the Transpolar Drift shifts eastward, aligning itself along the Alpha and Mendeleyev ridges (Plate 3b in Maslowski et al. 2000). The difference between the two 2-year mean ice velocity fields illustrates a basin-wide cyclonic trend (Fig. 1a in Maslowski et al. 2001). Figures 1a–c show equivalent 9-km model results for the 2-year mean sea ice drift of 1981–82 and 1991–92 and the difference between them. The general large-scale ice circulations and the decadal shift between the two 2-year means are similar to results from the previous model.

A significant difference exists in the Chukchi and southern Beaufort Seas in 1991–92, where the flow is anticyclonic in the 18-km model but cyclonic in the 9-km model (Fig. 1b). The 18-km model shows a much stronger southward flow over the Chukchi Sea towards Bering Strait in the 1980s compared to the 9-km model (Fig. 1a). Since both models use the same ECMWF forcing, we attribute these differences to the upper ocean dynamics, which are strongly affected by the flow of Pacific Water northward through Bering Strait, then eastward along the Chukchi and Beaufort shelves. The 9-km model predicts net mean northward flow through the open Bering Strait on the order of 0.7–0.8 Sv (McClean et al. 2001), in good agreement with observations (Roach et al. 1995). The 9-km model also yields more realistic shelf and boundary ocean currents in this region, which through ice–ocean drag affect the ice motion. From this analysis we conclude that spatial resolution does not significantly improve results from the old sea ice model, except indirectly through coupling of a more realistic ocean to sea ice.

The old model has a reasonable ice thickness distribution (Fig. 1d), but we find problems in

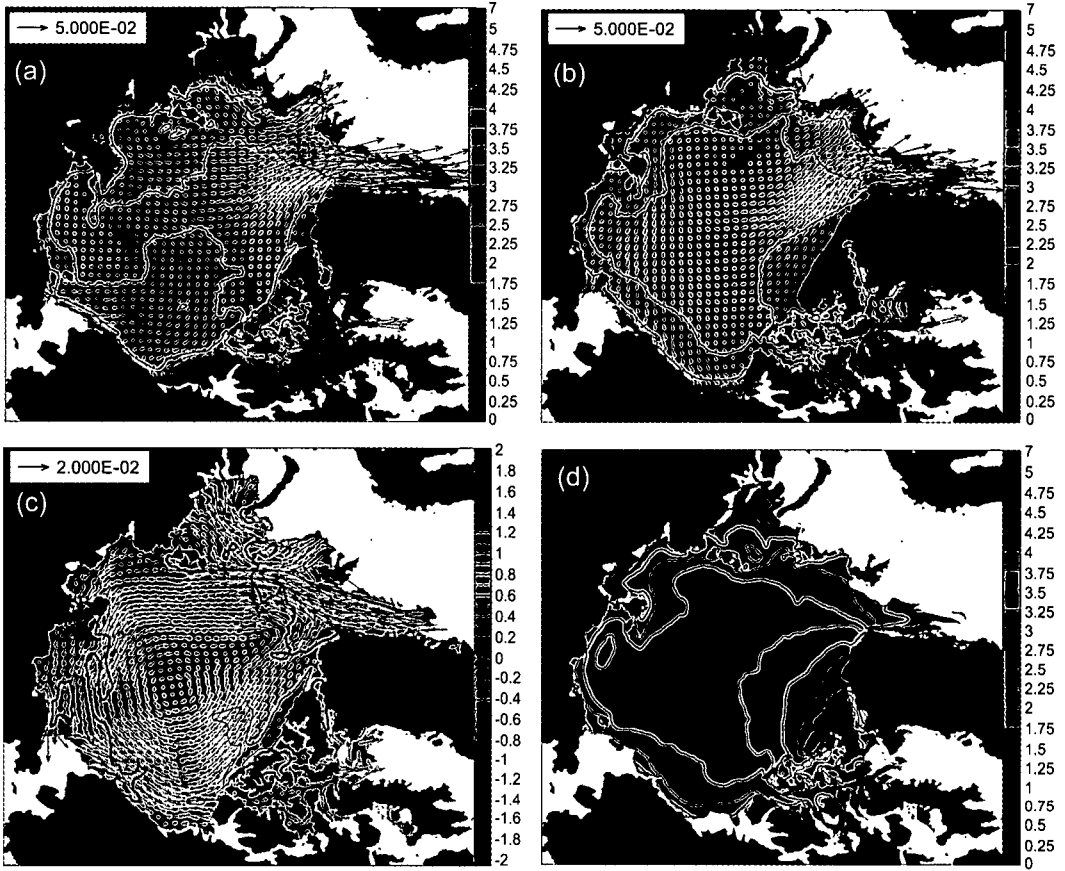


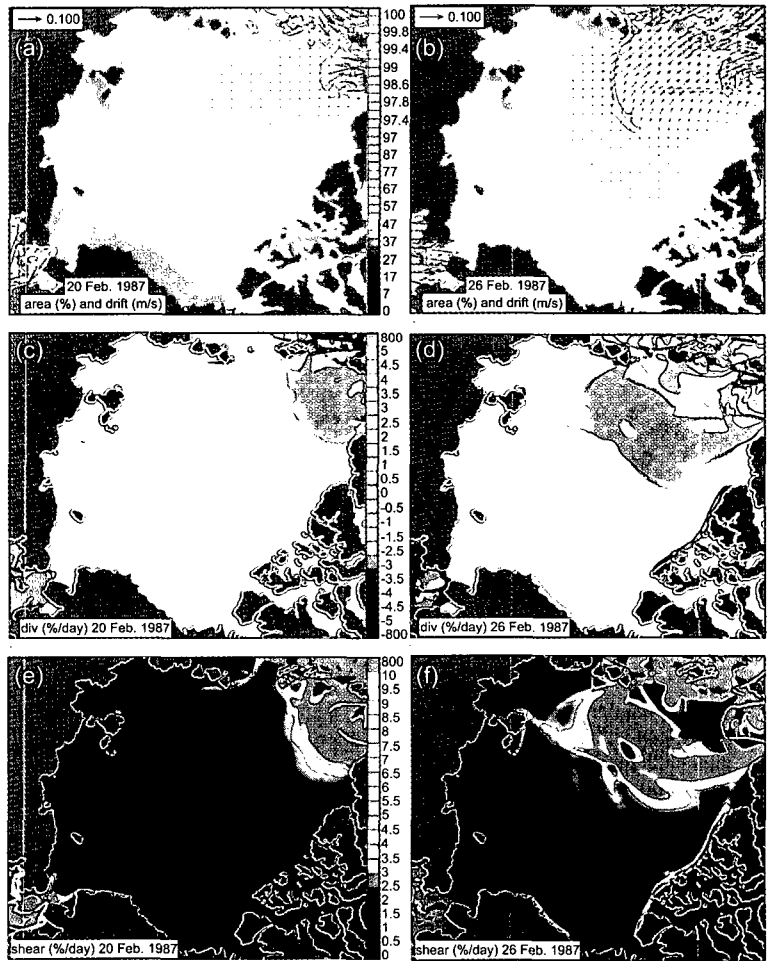
Fig. 1. The mean sea ice thickness distribution (m) and drift (m/s) for (a) 1981–82, (b) 1991–92, (c) the difference between 1991–92 and 1981–82, and (d) the 1979–1993 mean. Thick contour lines show the ice thickness every 1 m between 1 and 5 m. Thin contours in (d) are every 1 m between 0.5 and 4.5 m

the velocity and deformation fields. Figure 2 shows snapshots of ice concentration and drift (2a, b), divergence (2c, d), and shear (2e, f) from the old ice model. These snapshots are taken six days apart to show the response to a synoptic-scale change in atmospheric forcing. We chose results from mid-winter 1987 to maximize the influence of the internal ice stress and to avoid a bias toward either the cyclonic or anticyclonic atmospheric regime. The left and right columns show fields for 20 and 26 February 1987, respectively. Compared to buoy-measured ice speeds (<http://iabp.apl.washington.edu/>), which are typically in the range of 0–10 cm/s in the central Arctic, the ice speeds are too small. Large portions of the winter ice pack are almost completely still, even with ice–ocean drag present. The shear and divergence fields lack the long, narrow features seen in RGPS data. Instead, most of the

action takes place in large diffuse patches of high positive divergence and shear.

Figure 3 shows corresponding fields for the new ice model. In Fig. 3a and b, ice speeds in most of the Arctic basin are an order of magnitude larger than in the old model, in good agreement with buoy measurements. The anticyclonic Beaufort Gyre is present in buoy data for February 1987, though not as strong as in the plot from 20 February. (The model skill validated against buoy motions on a particular day depends strongly on the quality of the smoothed, coarse resolution atmospheric forcing.) A significant change in large-scale ice drift over 6 days suggests a strong dependence on synoptic-scale winds. The model ice concentration in the central Arctic is close to 100% as expected. The divergence and shear fields show long, narrow features with sharp gradients, which are qualitatively similar to RGPS

Fig. 2. Snapshots of (a, b) the total sea ice concentration (%) and drift (m/s), (c, d) sea ice divergence (%/day), and (e, f) shear (%/day) on (left) 20 February and (right) 26 February 1987 from the coupled ice–ocean model with the “old” sea ice model. Unit drift vector is 0.1 m/s.



observations (Kwok 2001). Upon closer comparison of high resolution SAR imagery to model deformation features, we find the model features to be wider and less frequent in space and time. We hypothesize that the model spatial resolution is insufficient to resolve the finer features measured with RGPS. Nevertheless, the “new” sea ice model shows dramatic improvements compared to the old model. We offer possible explanations in the next section.

Discussion and conclusions

The 18-km and 9-km “old” sea ice models have similar skill in representing the climate regime shift in the Arctic Ocean from the early 1980s to the early 1990s. The similarity in ice drift between the two models suggests that increas-

ing the model resolution has little effect on the ice strength. (One might have predicted that the ice strength and resulting drift would change due to increased resolution of fine-scale features such as leads.) There are some improvements in the representation of ice edge position, polynyas, concentration and thickness compared to lower resolution sea ice models (not shown). However, many of the improvements, such as the ice edge position in the Nordic and Bering/Chukchi seas, are influenced by more realistic modelling of the ocean currents and hydrography at increased resolution.

The old ice model gives ice speeds that are too small, despite having produced reasonable velocity fields in other studies, including Hibler (1979). In this study the mean ice thickness is 3–4 m in the central Arctic, giving an ice strength P of the order of 10^5 N/m during winter when the open water fraction is small. In Hibler

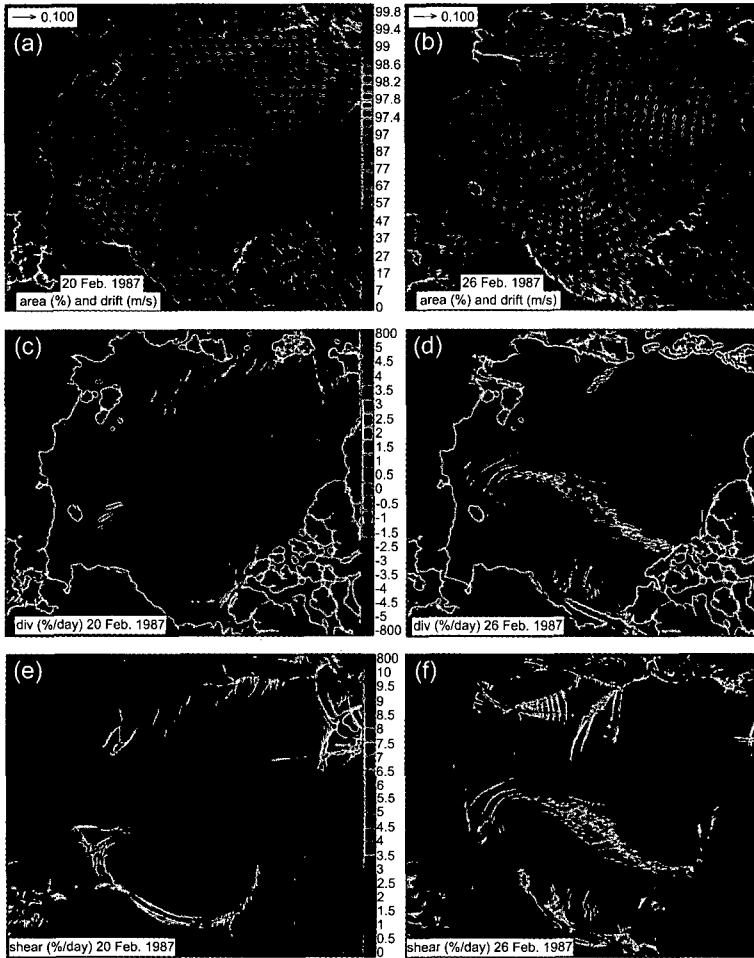


Fig. 3. Snapshots of (a, b) the total sea ice concentration (%) and drift (m/s), (c, d) sea ice divergence (%/day), and (e, f) shear (%/day) on (left) 20 February and (right) 26 February 1987 from the stand-alone “new” sea ice model. Unit drift vector is 0.1 m/s.

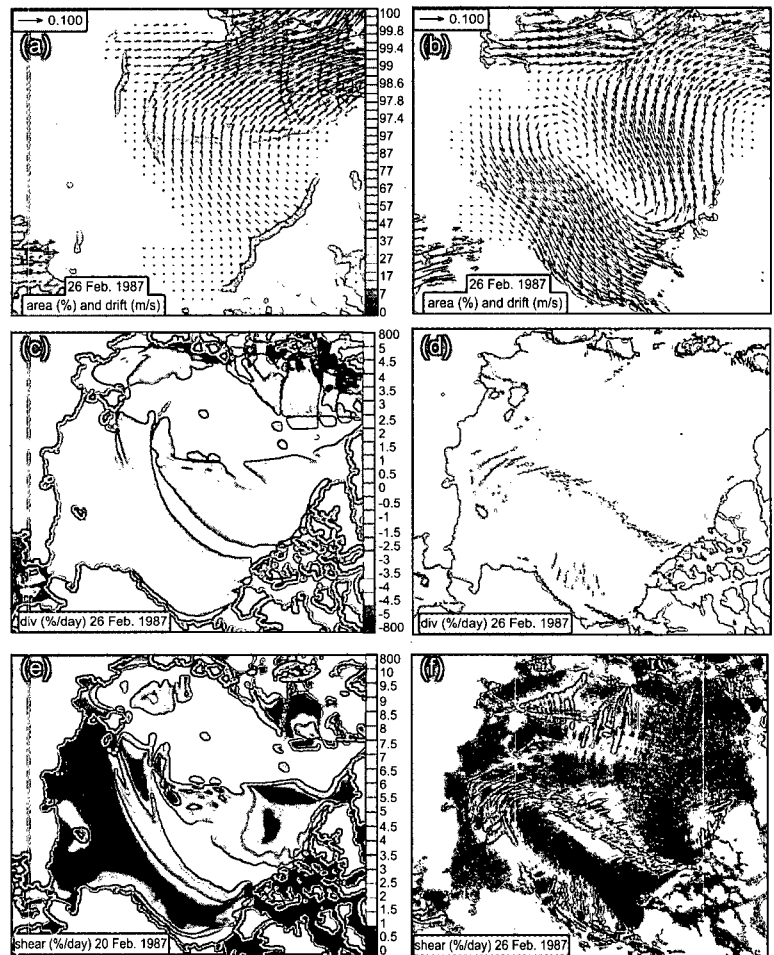
(1979) most of the ice was thinner than 3 m, giving much lower ice strengths. As shown by Steele et al. (1997), the ice motion field is a highly nonlinear function of ice strength. These authors found that ice moves at reasonable speeds when the average strength P is about 3×10^4 N/m, but rapidly locks up as the strength is increased. The mean ice thickness in our study is somewhat larger than observed, possibly due to biases in the atmospheric forcing.

To test the sensitivity of the velocity and deformation fields to the mean ice thickness, we repeated the simulation for the first two months of 1987—but with the ice thickness cut in half on 1 January, giving a thickness of less than 2 m in most of the Arctic. The resulting fields for 26 February are shown in Fig. 4a, c and e, which should be compared to Fig. 2b, d and f. Ice speeds are generally much larger, though still low on the

Pacific side of the Arctic. We obtained similar results for 20 February (not shown). We conclude that the ice strength and resulting drift in the old model are very sensitive to the mean ice thickness. The value of the strength parameter P^* could be lowered to give more realistic velocities in the presence of thicker ice, but we would prefer to avoid such arbitrary tuning. The deformation fields do not improve significantly when the ice is weaker and flowing faster. These fields have more structure over a larger region but are still very diffuse.

The new sea ice model yields more realistic velocity and deformation fields than the old model. Moreover, these fields are not very sensitive to the mean ice thickness. We repeated the above sensitivity test with the new model, halving the ice thickness in each category on 1 January 1987, then transferring ice to thinner categories

Fig. 4. Snapshots of (a, b) the total sea ice concentration (%) and drift (m/s), (c, d) sea ice divergence (%/day), and (e, f) shear (%/day) from sensitivity runs with reduced sea ice thickness by 50% from (left) the coupled ice–ocean model with the “old” sea ice model and from (right) the stand alone “new” sea ice model on 26 February 1987. Unit drift vector is 0.1 m/s.



as necessary. The resulting fields on 26 February are shown in Fig. 4b, d and f, which should be compared with Fig. 3b, d and f. Although there are small local differences, the overall similarity of the two sets of fields is striking. This is also true for 20 February (not shown). The similarity can be explained as follows. In the new ice model the ice strength depends not on the mean ice thickness \bar{h} but on the thickness of ridging ice h_r . (More precisely, the ice strength is proportional to the increase in potential energy during ridging, which itself is roughly proportional to the square of the mean ridge thickness. The mean ridge thickness in turn is proportional to the square root of h_r in each ridging category, following Hibler [1980].) Only ice in the thinnest 15% of the thickness distribution—mainly new first-year ice—contributes to ridging. Although the ice thickness is halved initially, within a few weeks

the thin ice categories have nearly the same ice area fraction and thickness as in the control run. As a result, the ice strength is almost unchanged.

If it is true that the strength of sea ice depends primarily on the amount and thickness of thin ice, then the behaviour of the new, multi-category ice model is much more realistic than that of the old, two-category ice model. Also, the new model is less likely to require special tuning for different atmospheric and ocean forcing. Imagine, for example, a climate change that increases summer melting without altering winter growth. The resulting ice would be thinner on average, but its winter ice strength would be about the same. The new model, unlike the old model, could capture this change accurately.

One suspected bias in the ice thickness fields of the new model is the build-up of thick ice along the Siberian coast (not shown), instead of along

the Canadian archipelago and Greenland as in the old model (Fig. 1) and in submarine sonar observations (e.g. Bourke & Garrett 1987). (We note, however, that relatively few ice thickness observations are available along the Siberian coast.) This bias may result, in part, from setting the ocean velocity to zero in the momentum equation. The winds were primarily toward Siberia in the months before February 1987, and ice in the uncoupled new model probably responds too strongly to winds. The spatial pattern of ice thickness will likely improve when the ice model is coupled to an ocean model. We will then be able to make a more definitive comparison between the ice concentration, thickness and velocity fields of the old and new models.

The most encouraging result from the new model is the high degree of realism in the ice deformation fields. The combination of high resolution with EVP dynamics, multiple ice thickness categories, and realistic ice strength produces shear and divergence fields similar to those derived from RGPS data. Despite known simplifications in the EVP model—for instance, the assumptions of isotropy and a normal flow rule—the rheology succeeds in reproducing features that extend hundreds of kilometres across the Arctic basin and vary on synoptic time scales. Although multi-decade integrations at higher resolution are not computationally feasible at present, we plan to repeat these experiments for shorter time periods or over a smaller region, to see whether deformation features become more realistic as the grid scale approaches the size of individual floes.

Acknowledgements.—This research was supported in part by the Dept. of Energy Climate Change Prediction Program (W. M. and W. H. L.), the National Science Foundation Arctic System Science Program (W. M.) and the Office of Naval Research High Latitude Dynamics Program (W. M.). Computer resources were provided by the Arctic Region Supercomputing Center and the US Army Engineer Research and Development Center through the Dept. of Defense High Performance Computer Modernization Program Grand Challenge Project.

References

Bitz, C. M., Holland, M. M., Weaver, A. J. & Eby, M. 2001: Simulating the ice-thickness distribution in a coupled climate model. *J. Geophys. Res.* 106(C2), 2441–2463.
 Bitz, C. M. & Lipscomb, W. H. 1999. An energy-conserving thermodynamic sea ice model for climate study. *J. Geo-*

phys. Res. 104(C7), 15 669–15 677.
 Bourke, R. H. & Garrett, R. P. 1987: Sea ice thickness distribution in the Arctic Ocean. *Cold Reg. Sci. Technol.* 13, 259–280.
 Bryan, F. O., Kauffman, B. G., Large, W. G. & Gent, P. R. 1996: *The NCAR CSM flux coupler. Technical Note TN-425+STR.* Boulder, CO: National Center for Atmospheric Research.
 Hibler, W. D. 1979: A dynamic thermodynamic sea ice model. *J. Phys. Oceanogr.* 9, 817–846.
 Hibler, W. D. 1980: Modeling a variable thickness sea ice cover. *Mon. Weather Rev.* 108, 1943–1973.
 Hunke, E. C. & Dukowicz, J. K. 1997: An elastic-viscous-plastic model for sea ice dynamics, *J. Phys. Oceanogr.* 27, 1849–1867.
 Hunke, E. C. & Lipscomb, W. H. 2001: *CICE: the Los Alamos sea ice model, documentation and software user's manual. LACC-98-16 v.3.* Los Alamos National Laboratory, NM.
 Jakobsson, M., Cherkis, N., Woodward, J., Coakley, B. & Macnab, R. 2000: A new grid of Arctic bathymetry: a significant resource for scientists and mapmakers. *EOS Trans.* 81(9), 89, 93, 96.
 Kwok, R. 2001: Deformation of the Arctic Ocean sea ice cover between November 1996 and April 1997: a qualitative survey. In J. Dempsey & H. H. Shen (eds.): *IUTAM symposium on scaling laws in ice mechanics and ice dynamics.* Pp. 315–322. Dordrecht, Netherlands: Kluwer Academic Publishers.
 Lipscomb, W. H. 2001: Remapping the thickness distribution in sea ice models. *J. Geophys. Res.* 106(C7), 13 989–14 000.
 Lipscomb, W. H. & Hunke, E. C. Unpubl. ms: Modeling sea ice transport using incremental remapping.
 Maslowski, W., Marble, D. C., Walczowski, W. & Semtner, A. J. 2001: On large-scale shifts in the Arctic Ocean and sea-ice conditions during 1979–1998. *Ann. Glaciol.* 33, 545–550.
 Maslowski, W., Newton, B., Schlosser, P., Semtner, A. J. & Martinson, D. G. 2000: Modeling recent climate variability in the Arctic Ocean. *Geophys. Res. Lett.* 27, 3743–3746.
 Maykut, G. A. 1982: Large-scale heat exchange and ice production in the central Arctic. *J. Geophys. Res.* 87(NC10), 7971–7984.
 McClean, J., Maslowski, W. & Maltrud, M. 2001: Towards a coupled environmental prediction system. In V. N. Alexandrov et al. (eds.): *Computational science—ICCS 2001: international conference, San Francisco, CA, USA, May 28–30, 2001: proceedings. Part 1.* Pp. 1098–1107. New York: Springer Verlag.
 Roach, A. T., Aagaard, K., Pease, C. H., Salo, S. A., Weingartner, T., Pavlov, V. & Kulakov, M. 1995: Direct measurements of transport and water properties through Bering Strait. *J. Geophys. Res.* 100(C9), 18 443–18 457.
 Rothrock, D. A. 1975: Energetics of plastic-deformation of pack ice by ridging. *J. Geophys. Res.* 80(33), 4514–4519.
 Smith, R. D., Dukowicz, J. K. & Malone, R. C. 1992: Parallel ocean general circulation modeling. *Physica D* 60, 38–61.
 Steele, M., Morley, R. & Ermold, W. 2001: PHC: a global ocean hydrography with a high quality Arctic Ocean. *J. Clim.* 14, 2079–2087.
 Steele, M., Zhang, J., Rothrock, D. & Stern, H. 1997: The force balance of sea ice in a numerical model of the Arctic Ocean. *J. Geophys. Res.* 102(C9), 21 061–21 079.
 Thorndike, A. S., Rothrock, D. A., Maykut, G. A. & Colony, R. 1975: The thickness distribution of sea ice. *J. Geophys. Res.* 80(33), 4501–4513.